ANALYSIS OF HALO FORMATION IN A DC PHOTOINJECTOR

D. Mihalcea, P. Piot, Northern Illinois University, DeKalb, IL 60115, USA

Abstract

We discovered, by modeling the AES/JLab direct-current photoinjector with several beam-simulation codes, that nominal injector settings would create a large diffuse beam halo as a consequence of the internal space-charge force in the beam. The injector-induced halo is sensitive to the injector settings, but if the settings are judiciously chosen, it can be largely circumvented. We present an exploration of the parameter space for the AES/JLab photoinjector. Measurement of beam halo will be a crucial aspect of commissioning this machine.

INTRODUCTION

The present driving accelerator for the Jefferson Lab 10 kW IR Free-Electron Laser (FEL) provides a 10 mA average current electron beam with energy up to 160 MeV and normalized transverse emittance less than 30 μm [1, 2]. Since the gain of the laser increases with the electron beam current [3], to achieve megawatt-class FELs the injector should be upgraded to increase the average beam current at ampere level.

The normalized transverse emittance scales linearly with the laser wavelength and the relativistic factor γ [4]:

$$\epsilon_N < \frac{\lambda \gamma}{4\pi} \qquad (1)$$

Shorter laser wavelengths and/or more compact driving accelerators (lower energy) can be achieved by decreasing the emittance.

The next generation megawatt-class JLab FEL will require much improved quality of the electron beam. In particular the average beam current must be at ampere level and the transverse emittance not larger than a few microns. The upgraded photoinjector was designed at Advanced Energy Systems (AES) [5] and will be fabricated at Jefferson Lab.

In this paper we present some simulation results for this upgraded AES/JLab photoinjector. Due to the relatively large space charge forces, there is the potential for unwanted halo formation. The goal of our annalysis is to determine what are the photoinjector operating conditions that preclude halo formation and maximize the beam quality.

AES/JLAB PHOTOINJECTOR

This new photoinjector [5] couples a normal-conducting DC gun a section of three 750 MHz superconducting RF single cells and a third harmonic 2250 MHz cavity. The schematic layout of the photoinjector is shown in Fig. 1.
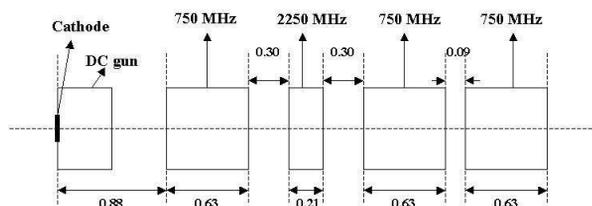

Figure 1: Schematic layout of the AES/JLab photoinjector. Emittance compensation solenoid is not shown. All dimensions are in meters.

Electron bunches of up to 1 nC charge and about 20 ps (rms) long are extracted from a photocathode illuminated with an infrared mode-locked Nd:YLF laser. The maximum accelerating gradient in the DC gun is 6 MV/m and the electron energy at the exit from the gun is about 1 MeV. At the end of the gun there is a solenoid to compensate the emittance growth due to space charge and external fields.

Three 750 MHz superconducting RF single cell cavities raise the energy of the electrons up to 6 MeV. A third harmonic cavity, located between first and second 750 MHz accelerating cavities, is used to linearize the energy dependence on longitudinal spatial coordinate.

BEAM HALO FORMATION

Photoinjector parameters like cavities amplitudes and phases, solenoid magnetic field, gun accelerating voltage are optimized to minimize longitudinal and transverse emittances at the exit from the photoinjector. Fig. 2 shows the most important beam moments when the charge of the electron bunches is 1 nC (750 mA), the initial beam radius at the cathode is 3 mm, and the initial longitudinal bunch profile is gaussian with $\sigma_z = 20$ ps.

The results from Fig. 2 were obtained with Parmela [6] and Impact-T [7]. The most sensitive parameters in the optimization process were the magnetic field in the emittance compensation solenoid and the phase of the third harmonic cavity. The values of the most important beam moments are within the desired limits when the current is 100 mA and about 20% higher for transverse and longitudinal emittances when the current is increased to 750 mA.

Beam halo may develop if the size of the laser spot at cathode is decreased in an attempt to increase the electron bunch charge density. Figure 3 shows the transverse beam distributions at two locations downstream of the cathode when initial distribution has radius 2 and 3 mm respectively, the beam current is 750 mA, and the laser pulse duration is 20 ps. When the initial radius is 2 mm the halo has
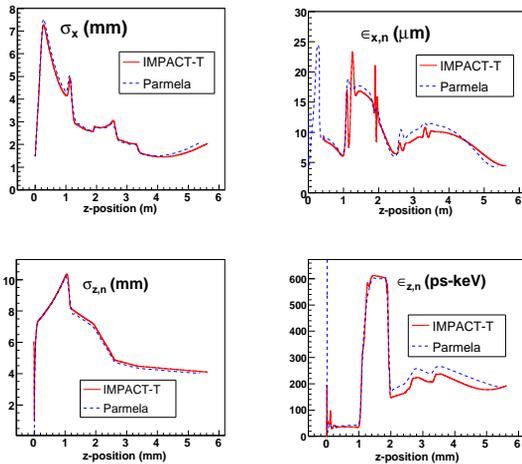
Figure 2: Beam moments as a function of the distance from the cathode. The average beam current is 750 mA and the radius of the beam at cathode is 3 mm.

Figure 4: The distance between the outermost particle and the beam axis (r_{max}), the radius of the beam (rms), and the normalized transverse emittance as functions of the beam radius at cathode.
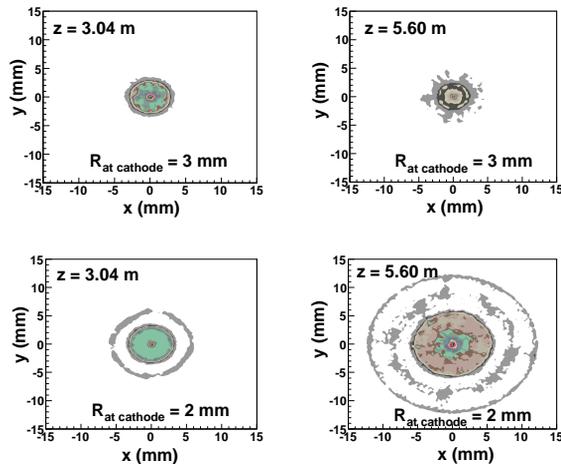

Figure 3: Transverse slices of the phase space at the entrance in the third accelerating cavity (left) and at the exit from the photoinjector (right). The radius of the beam at cathode was 3 mm (upper plots) and 2 mm (bottom plots).

the shape of cylindrical rings well separated from the core of the beam. There are two such rings at 5.62 m downstream of the cathode. The inner and outer rings contain 19% and 16% respectively, of the total bunch charge.

To identify the properties of the beam halo we tracked the outermost particles through the whole photoinjector. Figure 4 shows the distance between the outermost particle and beam axis, as well as beam radius and normalized transverse emittance as functions of laser spot size at the cathode. For 1 nC electron bunches halo may develop if laser duration is set at 20 ps and the initial transverse size is below 2.8 mm.

For the outermost particle (at the exit from photoinjector) Fig. 5 shows its radial position and velocity when ini-
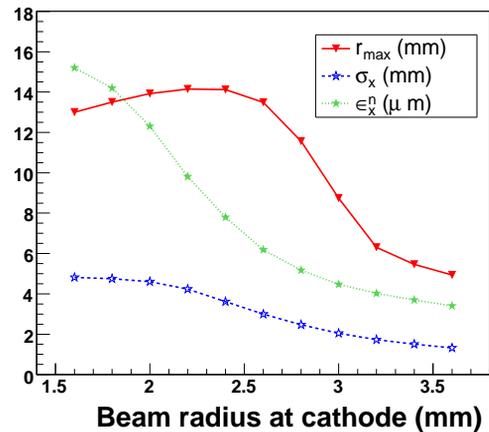
tial beam radius is 2 and 3 mm. For comparison, the non-realistic case when space charge forces are shutdown during the simulations is also shown in Fig. 5. When the spot size at the cathode is increased (from 2 mm to 3 mm) and the bunch charge is kept constant, the charge density decreases and consequently both radial electric field and radial velocity decrease. When space charge forces are turned-off there is still a small radial velocity (Fig. 5) due to the external electric field in the gun and accelerating cavities. The outermost particles at the exit from photoinjector (prime candidates for beam halo) originate from those particles that are farthest away from the beam axis at the generation level on the cathode's surface where space charge forces are maximal.

Our simulations show that transverse velocity and distance to beam axis are no longer linearly correlated when the initial beam radius is lowered to 2 mm. Figure 6 shows transverse velocity (in units of c) and distance from beam axis for all macroparticles when initial radius is 2 mm (upper plots) and 4 mm (bottom plots) and the z-location of the bunch is upstream (left plots) and downstream (right plots) of the first SRF cavity. Outermost particles have larger radial velocity moving toward the beam axis in the "2 mm" case (Fig. 6 top left plot) and they cross the beam axis after the reduction of the space charge forces due to the acceleration in the first SRF cavity (Fig. 6 top right plot). These particles, circled by the red marker in Fig. 6, break the laminar flow and depart from the core of the beam forming the ring-halo.

When the initial beam radius is increased from 2 mm to 4 mm (Fig. 6 bottom plots) the laminar flow is mostly restored but it is still true that the outermost particles originate from those with larger radial velocities at the entrance in the first SRF cavity.

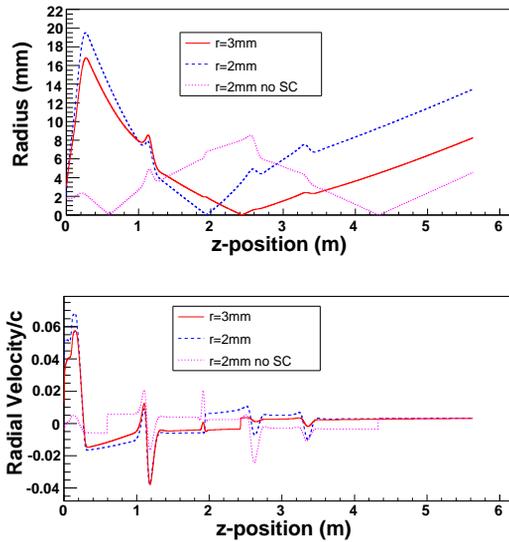By diminishing the space charge forces it is possible not

Figure 5: Top plot: the distance between the outermost particle and the beam axis as a function of the distance from cathode, when the initial beam radius was 2 mm, 3 mm, and 2 mm with space charge calculation turned off. Bottom plot: the radial velocity of the outermost particle as a function of the distance from cathode.
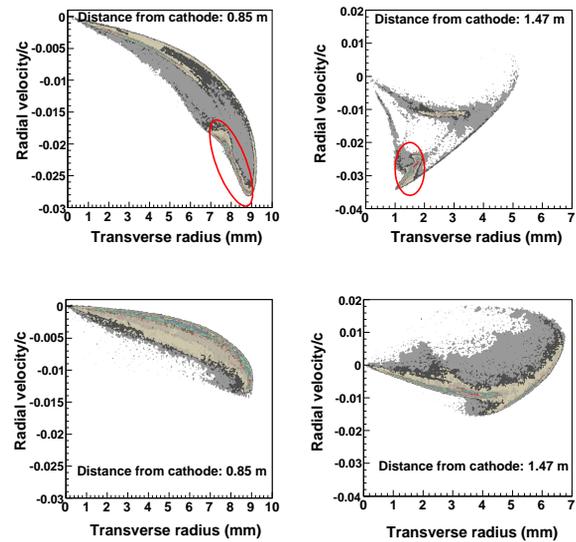
Figure 6: Slices of the phase space showing the radial velocity vs. the distance from the beam axis when the initial beam radius is 2 mm (upper plots) and 4 mm (bottom plots). For each case the plots correspond to two z-locations: upstream and downstream of the first SRF cavity. The red marker shows the location of the particles that generate the halo further downstream of the first SRF cavity.

only to improve the emittance but also to avoid the halo formation. In addition to increasing the laser spot at the cathode we investigated two more ways to reduce the space charge effects. The first was to use a flat longitudinal distribution (instead of the standard gaussian) [8] and the second was to use approximate ellipsoidal electron bunches [9]. Our simulations indicate that in both cases the halo formation can be avoided.

CONCLUSIONS

We determine as cause for halo formation in electron beams the early tidal shock from space charge forces. The particles that experience the largest radial space charge forces in the vicinity of the cathode are the source for beam halo.

The simplest way to suppress halo is to increase the laser spot size at cathode. In the case of AES/JLab direct-current photoinjector beam halo at the exit from the photoinjector may be present when 1 nC electron bunches are generated with transverse size shorter than 2.8 mm. Other techniques to lower the space charge forces, like the use of electron bunches with flat longitudinal distribution or ellipsoidal shape, can also suppress the beam halo.

REFERENCES

[1] D. Douglas, *et al.*, "A 10 kW IR FEL Design for Jefferson Lab", PAC2001, p249-252, (2001).

[2] C. Hernandez-Garcia, *et al.*, "Performance and Modeling of the JLab IR FEL Upgrade Injector", Proceedings of the 2004 FEL Conference, p558, (2004).

[3] C. W. Roberson and P. Sprangle, Phys. Fluids B **1**, p3, (1989).

[4] L. H. Yu, *et al.*, NIM A272, p436, (1988).

[5] A. Todd, *et al.*, Proceedings of 2003 IEEE Particle Accelerator Conference, Portland, OR, p977 (2003).

[6] L. Young, LANL report LA-UR-96-1835.

[7] J. Qiang, *et al.*, Proceedings of 2005 IEEE Particle Accelerator Conference (PAC 05), Knoxville TN, p 3316 (2005).

[8] R. Tikhoplav, *et al.*, Proceedings of the 2006 Advanced Accelerator Concepts, p 694-700 (2006).

[9] O. J. Luiten, *et al.*, Phys. Rev. Lett., vol. **93**, 094802 (2004).